INTERNATIONAL JOURNAL OF CIRCUITS, SYSTEMS AND SIGNAL PROCESSING
DOI: 10.46300/9106.2022.16.114 Volume 16, 2022

Research on the Enhancement Algorithm of Defocused and Blurred Image Base on Non-local Constraints

Erhui Xi*, Man Li
Guangzhou College of Technology and Business, Guangzhou, Guangdong, 528137, China

Received: March 30, 2021. Revised: February 25, 2022. Accepted: March 14, 2022. Published: March 30, 2022.

Abstract— Due to the diversity of defocus blurred images, causing the unsatisfied effect of sharpness enhancement of the defocused and blurred image. On this basis, the paper has proposed an enhancement algorithm of defocused and blurred image base on non-local constraints. The estimated results similar to the original image was acquired, the actual defocus blur optical transfer function was calculated and the low inverter over-amplifying the noise was avoided through the improvement of inverse filtering by the Wiener filter. Based on the symmetry of a defocused and blurred circular, the diffusion curve of straight marginal function was filtered and restored to eliminate the noise in the image. On this basis, the non-local self-similarity and total variational regularity of the defocused and blurred image were complemented, and the sharpness of the defocused and blurred image was finally enhanced by using the non-local model to restore the marginal and detailed texture information of the defocused and blurred image. The results of the simulation have shown that the proposed method could not only increase the computational efficiency, but also obtain satisfactory sharpness enhancement of the defocused and blurred image, and a better retain effect of the marginal information.

Keywords—Non-local constraint; defocus and blurred image; Transfer function; Wiener filter.

I. Introduction

The continuous development of informatization has created the conditions for the generation and flow of information. In the face of the explosive information growth capacity, people need to have a clear demand before acquiring information, containing the demand for information and information carriers, such as: text, graphics, video, etc., are information carriers, which are able to exist in the form of images, so it is clear that images are the main channel for people to obtain information sources. Through images people exchange information with each other, convey emotions, etc. In the information age, images are everywhere, such as street advertisements, web pictures, film and television images, paper books, etc., all involve a large number of images, and people spend a large proportion of their time on them every day.

Images are acquired in a variety of ways, and can be extracted from online resources or paper-based reading materials, and of course from real life. Images are acquired through camera equipment, with the help of electronic devices such as sensors, which often result in blurred images due to sensor defects, the external environment in which they are taken, resolution and other factors, making the images difficult to identify. There are also often out-of-focus images due to inaccurate focus, jitter and other reasons. With the advancement of optoelectronic technology and the emergence of autofocus technology, there is still insufficient autofocus accuracy and other multifaceted factors [1], making out-of-focus blurred images common, and out-of-focus image recovery has some research relevance.

II. Related research

As out-of-focus blurred images have caused people some trouble, some researchers have carried out research in order to make out-of-focus images relatively clear and easily recognisable to meet people's visual recognition ability, work and life needs.

For example, Jing Wenbo [2] and others analyzed the characteristics of simple optical imaging, established the point spread function model, and used the phase difference method to reconstruct the image and realize image enhancement; Cai Xiaoai [3] et al. Established an observation model to eliminate sequence spots in the image, reduce the influence of additive noise, and use the fuzzy kernel obtained by sparse constraint to realize image deblurring processing; Li Xuewei [4] et al. Used homomorphic filtering to preprocess the image, and then modified it with computer-aided tools. In order to obtain effective edge information of out of focus image and improve calculation efficiency. For this reason, an enhancement algorithm of defocused and blurred image base on non-local constraints was put forward. The estimated results similar to the original image was acquired, the actual defocus blur optical

transfer function was calculated and the low inverter over-amplifying the noise was avoided through the improvement of inverse filtering by the Wiener filter. Based on the symmetry of a defocused and blurred circular, the diffusion curve of straight marginal function was filtered and restored to eliminate the noise in the image. On this basis, the non-local self-similarity and total variational regularity of the defocused and blurred image were complemented, and the sharpness of the defocused and blurred image was finally enhanced by using the non-local model to restore the marginal and detailed texture information of the defocused and blurred image. The results of the simulation have shown that the proposed algorithm obtained satisfactory sharpness enhancement of the defocused and blurred image.

III. Sharpness enhancement algorithm of defocused and blurred image

A. De-noising of defocused image

Blurred images are formed in life for various factors, such as the motion of objects, defocus, increase of noise, etc. The paper focused on defocus. The process of defocus that blurs the image can be modelized to a function plus a noise term[5-11], the defocused and blurred image $f(x, y)$ was processed to form a degraded image $g(x, y)$.Given $g(x, y)$ and some knowledge about degenerate function H and the additional noise term $n(x, y)$, the approximate solution of the original image was obtained using its estimation, which was the key means of the enhancement of the defocused and blurred image. Therefore, the corresponding degraded image in spatial domain was obtained through the image degradation model as follows[12]:

$$g(x, y) = \begin{cases} H[f(x, y)] + n(x, y) \\ \int_{-\infty}^{+\infty}\int_{-\infty}^{+\infty} f(\alpha, \beta)h(x - \alpha, y - \beta)d\alpha d\beta + n(x, y) \\ f(x, y) * h(x, y) + n(x, y) \end{cases} \quad (1)$$

Where, the point spread function of the system was $h(x, y)$.To effectively simplify the calculation and keep the linear space unchanged, k_1 and k_2 were set as constants. $f_1(x, y)$ and $f_2(x, y)$ were two input functions, then the following formula was obtained:

$$H[k_1 f_1(x, y) + k_2 f_2(x, y)] = k_1 H[f_1(x, y) + k_2 f_2(x, y)] \quad (2)$$

$f(x, y)$ was set as a random input function , a and b were arbitrary constants, then:

$$H[f(x - a, y - b)] = g(x - a, y - b) \quad (3)$$

If formula (1) was Fourier transformed, the frequency domain expression could be expressed as:

$$\begin{cases} G(u, v) = F(u, v)H(u, v) + N(u, v) \\ F(u, v) = G(u, v) / H(u, v) - N(u, v) / H(u, v) \end{cases} \quad (4)$$

Where, $G(u, v)$ represented the Fourier transform of the defocused and blurred image; $F(u, v)$ represented the Fourier transform of the input function; $H(u, v)$ represented the transfer function of the imaging system .

The blurred image could be restored by inverse filtering if the defocused image was not disturbed by noise. However, the characteristics of inverse filtering resulted in its unsatisfactory effect of processing images. The following improvement of inverse filtering was effective, in which the simplest method was to directly perform the inverse filtering:

$$\widetilde{F}(u, v) = \frac{G(u, v)}{H(u, v)} \quad (5)$$

Wiener filter is linear, where the inverse filter was infinitely magnified to reduce the noise in the image. Therefore, taking the power spectrum of the image as priori knowledge, the Wiener filter $H_w(u, v)$ was used to minimize the mean square error E_2, then:

$$E_2 = \min E\left\{ [f(x, y) - \widetilde{f}(x, y)]^2 \right\} \quad (6)$$

Where, E was the expected value; the best estimated value of image $f(x, y)$ was $\widetilde{f}(x, y)$,and the restored image was obtained through the filter $H_w(u, v)$, among which the Wiener filter could be expressed[13-14] as:

$$H_w(u, v) = \frac{H*(u, v)}{|H(u, v)|^2 + s_{nn}(u, v) / s_{ff}(u, v)} \quad (7)$$

Where, $s_{ff}(u, v)$ represented the power spectrum of the defocused and blurred image; $s_{nn}(u, v)$ represented the power spectrum of external noise; $H*(u, v)$ represented the conjugate function of the transfer function $H(u, v)$ of the degenerate system. Since there was observation noise, $H(u, v)$ might equal to zero , while the denominator of

$H(u,v)$ would not be zero. Therefore, the negative affect caused by the inverse filtering was effectively constrained.

By using $H(u,v)$ to denoise, the formula was as follows:

$$\widetilde{F}(u,v) = \frac{H*(u,v)}{\left|H(u,v)\right|^2 + s_{nn}(u,v)/s_{ff}(u,v)} \times G(u,v) \tag{8}$$

Based on the above analysis, sampling and quantifying were carried out to $f(x,y)$ and the point spread function $h(x,y)$ to acquire the digitalized images and further acquire the discrete degradation model. Assume that the size of the original image was $M_1 \times N_1$, and the size of the point spread function was $M_2 \times N_2$, then f and h should be extended using the following formula, which was, to fill from zero to size $M \times N$:

$$f_e(m,n) = \begin{cases} f(m,n), 0 \le m \le M_1 - 1 \\ 0, M_1 \le m \le M - 1 \end{cases} \tag{9}$$

$$h_e(m,n) = \begin{cases} f(m,n), 0 \le m \le M_2 - 1 \\ 0, M_2 \le m \le M - 1 \end{cases} \tag{10}$$

The formation process of the defocused and blurred image could be described by formula (11) :

$$g = Hf + n = \begin{bmatrix} H_0, H_{M-1}, H_{M-2}, \ldots, H_1 \\ H_1, H_0, H_{M-1}, \ldots, H_2 \\ H_2, H_1, H_0, \ldots, H_3 \\ M, M, M, \ldots, M \\ H_{M-1}, H_{M-2}, H_{M-3}, \ldots, H_0 \end{bmatrix} \begin{bmatrix} f_e(0) \\ f_e(1) \\ f_e(2) \\ M \\ f_e(MN-1) \end{bmatrix} + \begin{bmatrix} n_e(0) \\ n_e(1) \\ n_e(2) \\ M \\ n_e(MN-1) \end{bmatrix} \tag{11}$$

The description of image degradation was a linear process, in which the following two points should be understood:

(1) Simulation results could be generated by using the description of the degradation process.

(2) The description of the degradation process could effectively constrain the noise of the image.

Assume that n was zero or the noise was unknown, then the denoising problem of the defocused and blurred image could be viewed as a least squares problem. Setting the objective function to minimum and then:

$$W(\hat{f}) = \begin{cases} \left\|e(\hat{f})\right\|^2 \\ \left\|g - H\hat{f}\right\|^2 \\ (g - H\hat{f})^T (g - H\hat{f}) \end{cases} \tag{12}$$

The parameterized Wiener filter could be accurately obtained through the matrix Fourier transform as follows:

$$W_c(u,v) = \frac{H*(u,v)}{\left|H(u,v)\right|^2 + \gamma p_n(u,v)/p_f(u,v)} \tag{13}$$

On this basis, the circular symmetry of the defocused image was used to obtain the defocus diffusion function, and the image was restored to eliminate the noise in it.

B. Enhancement of defocused images based on non-local constraints

Taking the denoise process of the defocused and blurred image as the research object, the total variation (TV) [15-18] model was used for constraint through the L^1 norm to effectively retain the marginal information of the image. The following energy functional could be obtained from the TV model:

$$E(u) = \iint_\Omega \left|u^0 - h*u\right|^2 d\Omega + \alpha \iint_\Omega \left|\nabla u\right| d\Omega \tag{14}$$

Where the Eular-Largrance equation was:

$$div\left(\frac{\nabla u}{|\nabla u|}\right) - \alpha.h*\left(h*u - u^0\right) = 0 \tag{15}$$

Where, u represented the curvature of the defocused and blurred image. To avoid zero divisor, generally, $\sqrt{\left|\nabla u\right|^2 + \varepsilon}$ was used to substitute $\left|\nabla u\right|$; When ε was not zero, however, some marginal and detailed information were smoothed out, thus ε was close to 0, and exact solutions were not able to be obtained.

When the defocused and blurred image was transformed by formula (15), its overall change was not solely decided by the corresponding level set, but also the grayscale of the image. With the increase of TV iterations, the grayscale of the image would approach a constant value.

To solve the smooth problem of the marginal and detailed information, norm in the TV model could be substituted by norm L^2. Meanwhile, the TV regularization degenerated into Tikhonov, making the image clearer.

The non-local model (NLM) used the implied information of the image to benefit the restore of the details, and specified the weight of a pixel according to the overall distribution of the grayscale of the image.

For each image block X_i, its similar block $X_{i,j}$ was searched in the observed image X. Assuming that $\|X_i - X_{i,j}\|^2 \le t$, then $X_{i,j}$ was the j th similar image block of X_i. $X_i^{'}$ was set as the center of X_i, $X_{i,j}^{'}$ the center of $X_{i,j}$, and F_{NLM} was the weighted $X_{i,j}$ to mainly predict the value of X_i, then:

$$F_{NLM}(X_i^{'}) = \sum_{j}^{n} \omega_{i,j} X_{i,j}^{'} \quad (16)$$

The weight $\omega_{i,j}$ was calculated as follows:

$$\omega_{i,j} = \frac{1}{c_i} \exp\left(\frac{d_{i,j}^2}{h^2}\right) \quad (17)$$

Where, $d_{i,j} = \|X_i - X_j\|$ represented the distance between the image block X_i and X_j, h was a constant that controls smoothness; c_i represented the normalized constant, which was:

$$c_i = \sum_{j=1}^{n} \exp\left(-\frac{d_{i,j}^2}{h^2}\right) \quad (18)$$

ω_i was set as a column vector with weight $\omega_{i,j}$, α_i represented a column vector containing pixel $X_{i,j}$, $\|X\|_{NLM}$ represented the regularization term of the non-local constraint, then:

$$\|X\|_{NLM} = \begin{cases} \sum_{X_i \in X}^{n} \|X_i - F_{NLM}(X_i)\|^2 \\ \sum_{X_i \in X}^{n} \|X_i - W_i^T \alpha_i\|^2 \end{cases} \quad (19)$$

Considering that there were a lot of redundant parts in the image, a smaller value was obtained through $\|X\|_{NLM}$ to restore more marginal information of the image. By introducing $\|X\|_{NLM}$ into the total variation image, then:

$$\hat{x} = \arg\min_{x} \left\{ \|y - Hx\|^2 + \lambda \|x\|_{TV} + \gamma \|x\|_{NLM} \right\} \quad (20)$$

After that, the classic iterative algorithm could be used to obtain the solution. The non-local self-similarity and total variational regularity of the defocused and blurred image were complemented to restore the marginal and detailed texture information of the defocused and blurred image, and the sharpness of the defocused and blurred image was finally enhanced.

IV. Simulation Experiment

After a theoretical derivation study, the original image (Figure 1(a)) was tested using a uniform software and hardware configuration. The comparative validation was carried out in an experimental environment under Windows with 16G RAM, 8-core CPU, and NVIDIA GeForce GTX 1650 Ti type graphics card with 4G video memory. The methods used in the comparison are: The method of this paper, Literature[3] method and Literature[4] method, and are compared in terms of experimental results, computational efficiency, and edge information protection. The experimental effect can visually determine the enhancement results of each of the three methods on the original image, the computational efficiency is analysed in terms of the execution speed of the three methods in the same configuration, and the execution efficiency of the methods is also an important indicator to be considered in the process of application promotion and research, and the edge information extraction can verify the effectiveness of the experimental effect on the image from the side.

（1）Experimental results

The method of this paper, Literature[3] method and Literature[4] method are used to enhance the sharpness of the original image, and the experimental results are shown in Figure 1. Figure 1(a) shows the original image, Figure 1(b) shows the enhancement effect of The method of this paper, Figure 1(c) shows the image sharpness enhancement effect of the Literature[3] method, and Figure 1(d) shows the image sharpness enhancement effect of the Literature[4] method.

(a) The original image

(b) The method of this paper

(c) The Literature[3] method

(d) The Literature[4] method

Figure 1. Image enhancement effect

As can be seen from Figure 1, there are four images in total, of which a represents the original image, which is a scene with the sky, sea and wood as the background. However, the white clouds, sea and wood are relatively vague, which seriously affects the identification of characters. The image looks like a mass of gray and unclear. If this type of image is not processed, it is an invalid image and has no meaning effect. After the enhancement of the three methods, Figure 1(c) and 1(d) are much clearer than the image a, and the edges of the sky, sea and wood are clearly distinguished. However, the wood and water surface in Figure 1(d) are still a little fuzzy, and the water lines cannot be seen on the water surface. The edge segmentation of the left wood and water surface is not clear, but the image c performs well in these aspects, and the edges between templates are clear. Figure1(b) is the image processed by the method in this paper. It can be seen that the edges of sky, sea and wood are clearly distinguished, the content of wood is more delicate, and the water lines on the water surface are clear and real. Through the processing of the original image in Fig. 1 (a) by three algorithms, the image definition is enhanced. Judging by human visual observation, the clarity of the image has been significantly improved by the method in this paper, and the effect is better than that of literature 3 and 4.

(2) Computational efficiency

The computational efficiency is analysed in the same configuration in terms of the execution speed of the three methods. The execution efficiency of the methods is also an important indicator considered in the application and research process, as shown in Table 1 for the three different methods.

Table 1. Computational efficiency

Number of Image Blocks	Computational Efficiency/%		
	The method of this paper	Literature[3] method	Literature[4] method
100	95.54	97.74	98.52
200	94.25	96.56	97.36
300	93.21	95.14	96.41
400	92.15	94.22	95.02
500	91.75	93.33	94.74
600	90.36	92.36	93.36

The calculation efficiency of the prepared pictures is tested in the hardware environment used in the simulation experiment. The three methods proposed in this paper, literature 3 method and literature 4 method are used to calculate respectively. The tested pictures are the same and the number is the same, and the calculation is carried out from 100 to 600. The test results are shown in Table 1. The efficiency of the three algorithms decreases with the increase of the number of pictures, It can be seen that the method in literature 4 has the highest execution efficiency and the algorithm proposed in this paper has the lowest execution efficiency, which is also the work to be done in future research to improve the execution efficiency of this method.

(3) Protection of marginal information

The integrity test of edge information protection is one of the methods to verify the effectiveness of image enhancement. Complete and effective edge information protection facilitates the recognition of images and reflects the effectiveness of the method from the side. To further verify the effectiveness of the this method, the retaining effect of marginal information of the defocused and blurred image have been tested using the three methods. Experiments were carried out on the margin of the original image, and the detailed results were shown in Fig.2:

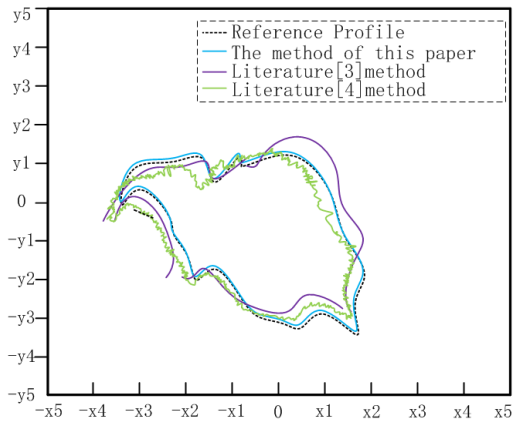

Figure 2. Margin test

As can be seen from Figure 2, the dotted line indicates the contour line of the image, the light blue line indicates the contour line of the image after processing by this method, the light green line indicates the contour line of the image after processing by the Literature[3] method, and the purple line indicates the contour line of the image after processing by

Literature[4] method. The method of this paper is able to render the image edge contours well, and basically matches the preset contour information, with some deviations in some places. The literature[3] method has more burrs, resulting in bulging image edges, while the edge processing of The literature[4] method is too rounded and there are breakpoints, so the edge information is not well retained.

V. Conclusion

With the application of intelligent image processing in various fields, people are having higher and higher demands for image quality. Since images were interfered by many factors, which bring noise to and blur them, making image enhancement extremely important[19-21]. To effectively solve the blur problem caused by defocus, an enhancement method of defocused and blurred image base on non-local constraints was put forward. The simulation experimental results show that the method of this paper, Literature[3] method and Literature[4] method are used to compare the experimental effect, computational efficiency and edge information protection in three aspects respectively. From the experimental results, all three algorithms achieve image sharpness enhancement for the original image processing in Figure 1(a). However, judging by observation with human eye vision, the clarity of the image was significantly enhanced after the method of this paper enhancement, and the effect was better than that of the Literature[3] and the Literature[4], and the the sky, sea and wood were more realistic. However, in terms of computational efficiency, the efficiency decreases with the increase of the number of pictures, but the computational efficiency of the algorithm proposed in this paper is poor. From the perspective of edge preservation, the method of this paper can better present the image edge contour, which is basically consistent with the preset contour information. The Literature[4] has many burrs, while the Literature[3] has too smooth edge processing and breakpoints.

Although the proposed method in the paper has achieved some results, however, more improvements need to be done due to the limitations of environment and human factors. Subsequent study will focus on the following two aspects:

(1) A more accurate degradation model will be established to obtain more satisfactory image enhancement effect;

(2) Corresponding evaluation indicators of the image enhancement effect will be set up to meet the sensory needs of human eyes;

(3) Improve the computational efficiency of this method.

References

[1] Wang Xu, Chen Qiang, Sun Quansen. Multichannel Spectral-Spatial Total Variation Model for Diffractive Spectral Image Restoration[J]. Journal of Computer Research and Development, 2020, 57(2):413-423.

[2] Jing Wenbo, Zou Huanhuan, Zhao Zhiyuan, etc. Simple Optical System Image Restoration Method Based on Phase Diversity[J]. ACTA PHOTONICA SINACA, 2019, 48(9):1-12.

[3] CAI Xiaoai, ZHANG Haimin. Multi-scale Deblurring Method for Defocused Image Based on Sparse Constraint[J]. Journal of Changshu Institute of Technology?Natural Sciences?, 2021,35(2):65-69.

[4] LI Xuewei, ZHANG Rui. Ship image enhancement method based on computer aided processing technology[J]. SHIP SCIENCE AND TECHNOLOGY, 2020,42(9A):64-66.

[5] MA Xiao-tao. Ship image enhancement based on homomorphic filtering[J]. SHIP SCIENCE AND TECHNOLOGY, 2020,42(3A):85-87.

[6] Wei Hao, Cui Haihua,Cheng Xiaosheng, etc. Image Defocus Simulation Technology Applied to Evaluation of Focused Morphology Recovery Algorithm[J]. Acta Optica Sinica, 2019, 39(11):1-9.

[7] Tong Ying. The Image Enhancement Algorithm Based on Retinex Filter Coupling Post-processing Optimization[J]. PACKAGING ENGINEERING, 2018, 39(15):227-236.

[8] Zhang Chi, Tan Nanlin, Li Xiang,etc. Foggy image enhancement technology based on improved ?etinex algorithm [J]. Journal of Beijing University of Aeronautics and Astronautics, 2019, 45(2):309-316.

[9] Chen Zheng. Design and implementation of infrared image detail enhancement algorithm based on FPGA [J]. LASER & INFRARED, 2018, 48(7):925-929.

[10] Chen Changhua, Liu Yu, Cui Qiang. Remote sensing image defog algorithm based on saturation operation and dark channel theory [J]. Computer Engineering and Applications, 2018, 54(5):174-179.

[11] Xu Jingtian, Feng Xin. Lossless restoration of digital media images based on ambiguity parameter estimation [J].
Journal of Xi'an Polytechnic University, 2019, 33(6):685-690.

[12] Wang Yuanyuan. Research and application of defocus blurred image processing[D]. Beijing: North China University of Technology,2011.

[13] Xie Jing. Study on Restoration Method of the Fuzzy Iris Image[D]. Changchun:Jilin University,2009.

[14] Wang Yanni, Yang Xiaobao. An Improved Algorithm of Image Dehazing Based on Sky Region Recognition [J]. Journal of Detection & Control, 2020, 42(2):71-78.

[15] Zhao Hui, Wei Weibo, Pan Zhenkuan, etc. Research on Image Dehazing Based on Dark Channel Prior and
Variational Regularization[J]. Computer Engineering, 2021, 47(10):214-220.

[16] Chang Huibin, Zhang Jie. Review of variational regularization method for mixed Poisson-Gaussian noise removal[J]. Journal of Tianjin Normal University(Natural Sciences Edition), 2020,40(4) :1-10.

[17] Tao Xingpeng, Xu Honghui, Zheng Jianwei, etc. Hyperspectral Image Denoising Based on Nonconvex Low Rank Matrix Approximation and Total Variation Regularization[J]. COMPUTER SCIENCE, 2021,48(8):125-133.

[18] Li Xiaolu, Zhou Yatong, He Jingfei, etc. Total variational regularization for non-local mean seismic data denoising[J]. Computer Engineering & Science, 2020,42(6):1106-1110.

[19] Jiang Hanqiong, Shen lei, He Jing, etc. Non-local Means Filtering Based on GLBP Constraint for Finger Vein Image Denoising[J]. Journal of Hangzhou Dianzi University(Natural Sciences), 2020, 40(6):32-36.

[20] Ma Wentu, Jiang Youyi, Li Xiao, etc. Denoising Method Combining Non-local Mean and Wiener Filter in Wavelet Domain[J]. Beijing Surveying and Mapping, 2019,33(9):1020-1024.
[21] Fan Peipei, Dong Xiucheng, Li Tao, etc. Super-Resolution Reconstruction of Depth Map Based on Non-Local
Means Constraint[J]. Journal of Computer-Aided Design & Computer Graphics, 2020,32(10) :1671-1678.